

Thermal characterization of composite materials for thermochemical heat storage for building applications

Julie Dussouillez¹, Benoit Michel¹, Kévy Johannes¹ and Frédéric Kuznik¹

¹ Université de Lyon, CNRS, INSA-Lyon, Université Claude Bernard Lyon 1, CETHIL UMR5008, F-69621, Villeurbanne, France

Abstract

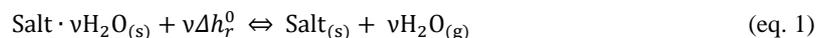
Nowadays, thermochemical storage systems show high theoretical energy performances and are even considered as more appropriated than sensible or latent storage systems, especially for long-term thermal storage. Nevertheless, in thermochemical reactor, agglomeration phenomenon caused by the formation of hydrates on the surface layer of the bulk salt usually occurs. To counteract this negative effect, composite materials composed by a porous matrix with impregnated salts are under investigation. The present contribution focuses on the LaCl_3 , which is one of the most promising salts, in order to provide a better understanding of its energetic properties. First studies were carried out at the salt crystal scale and then at larger scale of the thermochemical reactor with impregnated matrix. Studies of LaCl_3 crystal provide the thermodynamic equilibrium and the reactor scale highlights temperature distribution and humidity variations during storage/release of heat.

Keywords: Thermochemical Heat Storage, Hygroscopic Salt, Sorption, Desorption, Lanthanum Chloride.

1. Introduction

In a context of a progressive depletion of the world's fossil fuel reserves, researches are turning toward renewable sources, and more specifically solar energy. Solar is free, unlimited, abundant, greenhouse gas-free source of energy, it seems to be an excellent solution for heating buildings efficiently. However, because of the intermittent nature of the solar energy, heat storage and especially long-term thermal energy storage is no longer a possibility but a necessity, for building application.

There are several types of thermal heat storage systems. The most common are sensible and latent [1]–[3]. Nevertheless, due to their important thermal losses and storage volume, there are not the most appropriated for long-term heat storage. Thermochemical storage seems to be a good alternative to heat buildings sustainably and without heat loss. Thermochemical heat storage is based on the thermal effect of a monovariant reversible chemical reaction between a solid and a gas (eq.1). Two types of thermochemical systems exist: open and close systems. Open systems have been identified as the most promising for heat storage in building applications. In these systems, the reactive solid is crossed by a moist air flow at atmospheric pressure [4]. This paper focuses on hydrate/water pair, whose are the most promising pairs for building applications [5]–[7]:



The reaction is endothermic during dehydration and exothermic during hydration. The equilibrium condition (p_{eq} and T_{eq}) of the solid/gas reaction follows the Gibbs relation, expressed with the equation 2. ΔH_r represents the enthalpy of the reaction and ΔS_r , the entropy.

Gibbs equation:
$$p_{eq} = p^0 \cdot e^{\left(\frac{-\Delta h_r^0}{RT_{eq}} + \frac{\Delta s_r^0}{R}\right)} \quad (\text{eq. 2})$$

In thermochemical heat storage, energy heat is stored as a chemical potential form. it means that chemical reaction will be performed and heat will be released when the two materials will be associated. No thermal losses are expected as opposed to sensible or latent energies. The storage period can be as long as needed. Furthermore, thermochemical storage presents the advantage to have a high energy density, superior to those of the sensible and latent heat storage systems. The two storages mediums are hygroscopic salt crystals on one side and water on the other, as it is represented in Figure 1. In this heat storage system, heat stored is directly linked with: the amount of the storage material and the heat of reaction [8].

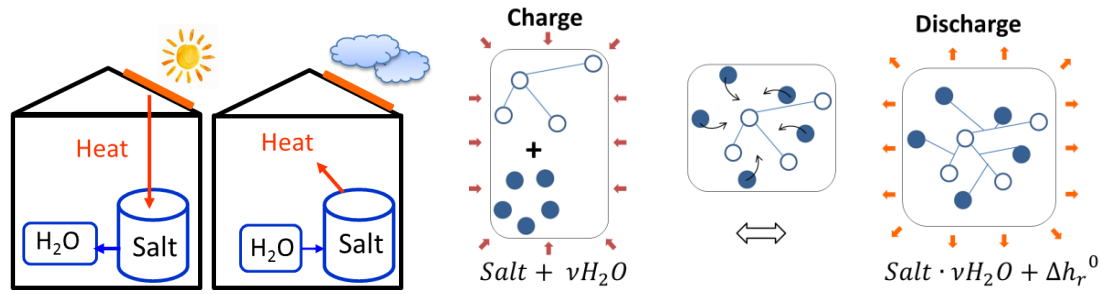


Figure 1: Thermochemical heat storage system in a house (left) and the reversible chemical reaction (right).

Thanks to its high theoretical performance, thermochemical heat storage is tending towards getting ahead of other energy storage systems as sensible or latent storages, especially for long term thermal storage [6]. However, as it is shown in Figure 2, all these devices are not at the same technology readiness level (TRL) and thermochemical storage system is still a not yet a mature technology [5]. As a matter of fact, sensible heat storage has the higher TRL.

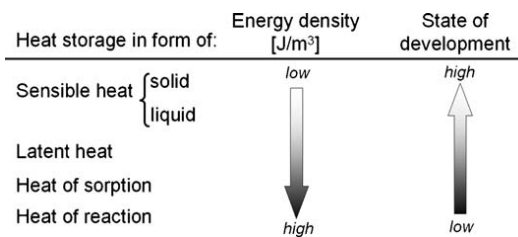


Figure 2: Energy density of physical and chemical changes [5]

Over the past decade, studies from different authors and countries have been carried out in order to determine the most promising hygroscopic salts hydrates for heat storage systems for building application. Indeed, several studies compared from ten to more than three hundred salts to each other using step-by-step screening. Some authors have only conducted experimental campaigns; while others like Richter et al. [11] have primarily carried out feasibility study based on theoretical analysis of thermodynamic data, and then achieved an extensive experimental analysis of the reversibility, reaction hysteresis and cyclability. A number of salts, with incompatible characteristics for building application (such as toxicity, corrosiveness, cyclability potential or operating and regeneration temperatures) were first removed from the list of potential candidates. Then, energy density or reversibility capacities were investigated for each remaining salts [7], [9]–[11]. Two recent studies carried out by N'Tsoukpoe et al. [10] and Richter et al. [11] showed similar results and identified strontium bromide (SrBr₂), magnesium sulphate (MgSO₄) and lanthanum chloride (LaCl₃) as the three most promising salts for thermal heat storage applications.

Unlike SrBr₂ and MgSO₄ which were the subject of a number of studies and investigations, LaCl₃ is not well-known and the literature dealing with this salt is limited. Most of the studies concerned its thermodynamic properties but some results differ from each other.

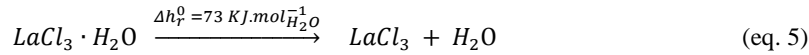
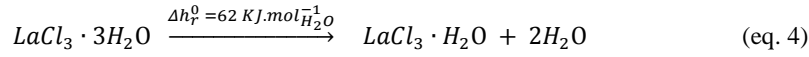
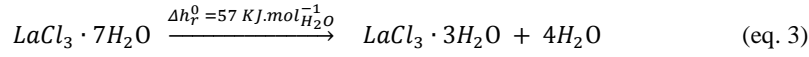
One of the main drawbacks of thermochemical systems is the implementation of the solid reactive material. Although packed bed of pure materials have been largely studied [1], this implementation presents many disadvantages, such as transfer limitation, performances degradation due to microstructure change, melting and aggregation after excess hydration [12], [13]. Salt hydrates can be confined into porous matrix to turn into composite reactive materials in order to overcome the aforementioned issues. They are composed by inorganic salts hosted in porous matrix, which can be active (zeolite, silica gel) or not (expanded graphite, or vermiculite) [12]. Recently, promising composite using honeycomb ceramics as a non-active porous matrix proved the feasibility of the concept [14]. However, a number of scientific and technical obstacles remain to be solved in order to characterize and optimize the heat and mass transfers, as well as the energy density of such composite.

This paper highlights studies of LaCl₃ for storage applications. The objectives of this work are to improve the understanding of LaCl₃ thermodynamic properties and to validate this salt as a promising candidate for heat storage systems for building applications. Two scales were studied. The first one focuses on the intrinsic properties of the hygroscopic salt with the definition of the thermodynamic equilibrium diagram, whereas the second deals with the larger scale of the thermochemical reactor by studying a non-active ceramic matrix with LaCl₃ salt hydrate impregnated.

2. Thermodynamic study of LaCl_3

2.1. State of art

LaCl_3 can be decomposed from lanthanum chloride heptahydrate to anhydrous form through three consecutive reactions, presented with the eq. 3, eq. 4 and eq. 5. The theoretical mass losses of each of the three dehydration reactions are 19.4wt%, 9.7wt% and 4.9wt% respectively, regarding the heptahydrate solid of LaCl_3 , which corresponds to a total mass loss of 34%wt.



Sahoo et al. [15] achieved an experimental campaign in order to evaluate some properties of the LaCl_3 , such as its enthalpy and entropy of reaction. They did their research by dehydration process from LaCl_3 heptahydrate to anhydrous form. Whereupon, they made a comparison between their work and two others studies. One experimental study, carried out by Polyachenok et al. [16] where the decomposition reactions were studied by creating each crystalline state one by one, from an aqueous solution. And one numerical study with a mathematical model [17], [18].

Figure 3 shows the evolution of the water vapor pressure as a function of the temperature for various studies from the literature. The first equilibrium from LaCl_3 heptahydrate to trihydrate is represented in blue. The second equilibrium is in orange and the last one in green. Figure 3 shows that the results from literature do not overlap, which evidence the need of further experimental results. Therefore an experimental campaign was conducted. Thermodynamic equilibriums were studied at a constant pressure set in dehydration process. For each water vapor pressure, three experimental points were identified by studying mass losses and heat flow variations.

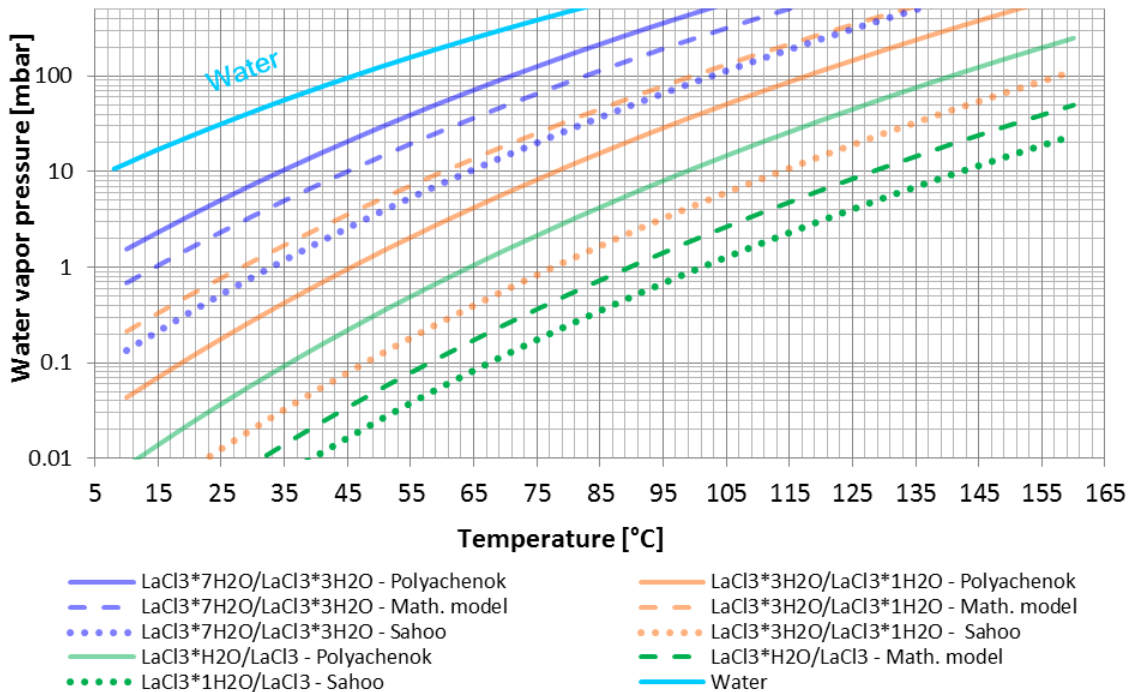


Figure 3 : Thermodynamic diagram on LaCl_3 – literature

2.2. Material and method

In order to define thermodynamic equilibrium state of LaCl_3 , some experimental campaigns were carried out by studying mass loss and heat stored during dehydration process. All these studies were based on Thermogravimetric Analysis (TGA) with SETARAM SENSYS Evolution, France instrument (TG-DSC). TGA characterization consists in measurement of sample mass variation compared to a reference while the temperature of the sample is programmed in a controlled atmosphere (i.e. temperature and water vapor pressure). Indeed, SETARAM Sensys Evolution TG analyzer has been coupled with SETARAM WETSYS controlled humidity generator. All our experimental analyses were carried out in flowing nitrogen controlled atmosphere (50 mL/min).

Thermodynamic analysis was carried out by dehydration process of LaCl_3 , from heptahydrate to anhydrous form. Each sample was prepared with about 3mg of crushed powder of hydrated lanthanum chloride and dehydrated at a constant pressure set (depending on the case studied) and a temperature gradient set from 20°C to 200°C. Three pressures sets were studied: 5mbar, 10mbar and 25mbar. For each samples, a first step was done (stabilization phase or preheating) at a constant pressure and temperature, in order to ensure that each salt hydrate samples was in the same initial conditions and so, same crystalline structures before starting dehydration process. Then, the second step is the 'dehydration phase'. During this phase, samples were heated up to 200°C with the constant heating rate of (0.05, 0.2 or 0.5K.min⁻¹ depending on the case studied). The lower the heating rate is, clear and precise the reaction steps are. Figure 4 explains the experimental protocol for the thermodynamic study of dehydration of this salt hydrate, from heptahydrate to anhydrous form. Because the crystalline state of the salt depends on its pressure and temperature, the stabilization temperatures of each sample were adjusted in order that salt crystals always stays in their heptahydrated state; i.e. in the $\text{LaCl}_3 \cdot 7\text{H}_2\text{O}$ form. For the sample studied at 5mbar, the stabilization was done at 30°C, then heated up to 200°C. The stabilization temperatures of the two others samples were 40°C and 50°C for 10 mbar and 25mbar respectively.

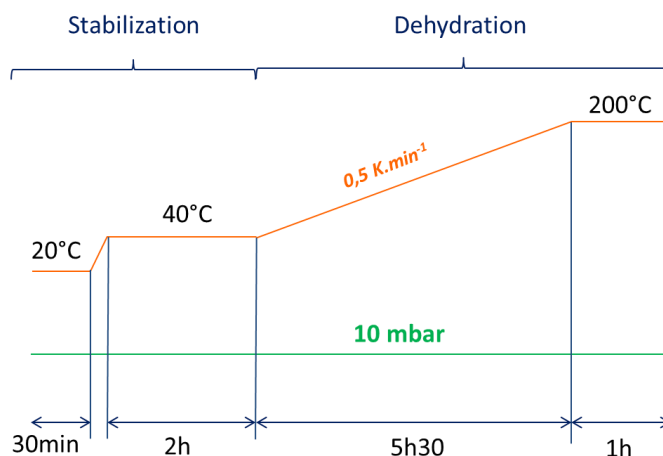


Figure 4: Evolution of the temperature and pressure sets - Thermodynamic study at 10mbar (LaCl_3)

Similarly to the well-known effect of shift of the melting and solidification peaks to low and high temperature for phase change material analysis by DSC (due to the high energy involved during phase change, inertia and heat transfer resistances inside the sample) [19], heating rate has an influence, which could be no-negligible, on the clarity of the results and the reading accuracies of the ATG-DSC results of the thermochemical reactions. Thus, some investigations were done for these three pressures studied. A first experimental campaign was carried out with the constant pressure of 10mbar for three different heating rates: 0.05, 0.2 and 0.5K.min⁻¹. Then, a second experimental campaign was carried out at 5mbar for two heating rates (0.2 and 0.5K.min⁻¹). For the last one, a sample of crushed LaCl_3 was studied at 25mbar and a heating rate of 0.5K.min⁻¹.

The onset temperature of each of the three-step reaction was considered at the intersection line between the beginning of the mass loss and the triggering of the endothermic peak, as it is represented in the Figure 5.

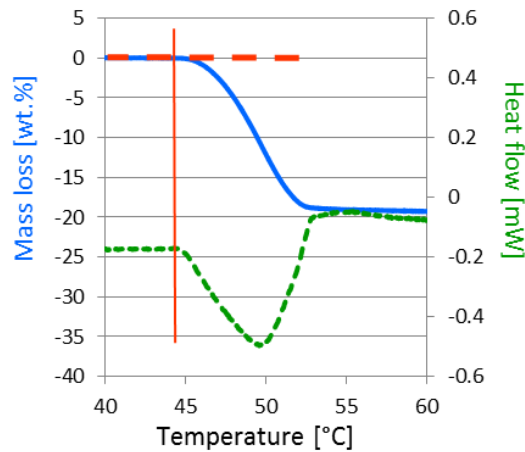


Figure 5: Determination of the onset temperature

2.3. Results and discussion

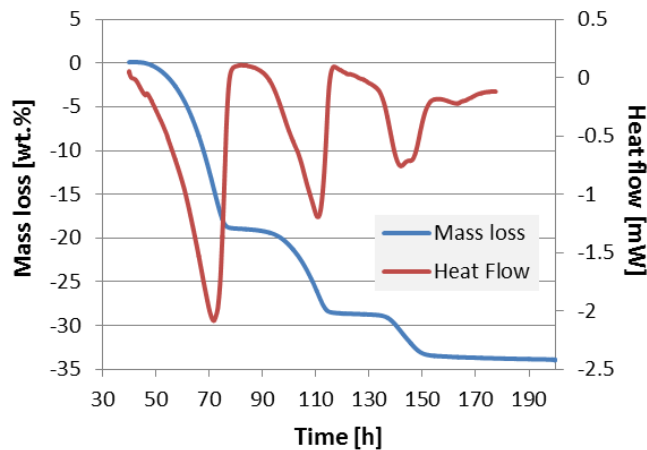


Figure 6: Mass loss and heat flow of a 3mg of LaCl_3 powder - Dehydration to 200°C at 0.5K/min and 10 mbar – ATG-DSC

Figure 6 presents the three reaction steps of dehydration of LaCl_3 characterized by three mass losses and three endothermic peaks. These results were obtained thanks to the experimental protocol described previously, at of 10mbar pressure set. The first dehydration step corresponds to 4 water molecules loss which represents 19.4%wt compared to the initial mass of solid hydrate. The second mass loss corresponds to the next two molecules of water for a percentage of mass loss equivalents to 12%wt. The last step is the loss of the seventh and the last water molecule (6.8%wt). Enthalpy of reaction can be found by studying the heat flow curve, which is characterized by an endothermic peak in dehydration process. Indeed, the stored heat is directly linked to the area of each endothermic peak. The values of enthalpy of reaction are given in Table 1 for each of the three decomposition reactions of LaCl_3 .

Table 1: LaCl_3 intrinsic characteristics: enthalpy and entropy of reaction – three reaction steps of LaCl_3

Reaction step	Mass loss [%wt]	Δh_r^0 [J/mol _{(H₂O)]}	Δs_r^0 [J/K]
$\text{LaCl}_3 \cdot 7\text{H}_2\text{O} \rightarrow \text{LaCl}_3 \cdot 3\text{H}_2\text{O} + 4\text{H}_2\text{O}$	19,4	57 000	142.6
$\text{LaCl}_3 \cdot 3\text{H}_2\text{O} \rightarrow \text{LaCl}_3 \cdot \text{H}_2\text{O} + 2\text{H}_2\text{O}$	12,0	62 000	137.5
$\text{LaCl}_3 \cdot \text{H}_2\text{O} \rightarrow \text{LaCl}_3 + \text{H}_2\text{O}$	6,8	73 000	149.8

Figure 7 presents the results obtained for the three dehydration steps of LaCl_3 , for three different heating rates. It can be noticed that the onset temperature of the dehydration is shifted to higher temperature when the heating rate increases. This precision and difference of reading is even more important for the last two step reactions. Indeed, for the last dehydration reaction, from LaCl_3 monohydrate to anhydrous form, the onset temperature read is about 129°C at 0.5K.min⁻¹, whereas it is 117°C at 0.05K.min⁻¹, then a difference of 12°C when the heating rate is divided by 10. The heating rate has therefore a relatively influence on the onset temperature, and it can be noticed that it is linear. So, by connecting the three experimental points for each of the three reaction

steps, we can obtain the ‘real’ onset temperature by considering the heating rate of $0\text{K}\cdot\text{min}^{-1}$. Nevertheless, the slope is not identical for the three chemical reactions. In order to confirm and validate these results, a second experimental campaign was carried out at 5mbar and with the two heating rate: 0.2 and $0.5\text{K}\cdot\text{min}^{-1}$ (‘real’ onset temperature obtained were presented in the Table 2. Results were conclusive and close to the 10mbar pressure ones with different heating rate. The ‘real’ onset temperatures (at $0\text{K}\cdot\text{min}^{-1}$) were deduced for 5mbar from this second experimental campaign. Moreover, results obtained at 25mbar were extrapolated thanks the slope of the two other and the lasts ‘real’ onset temperatures were defined. Those ‘real’ onset temperatures from the three experimental points of each reaction steps were represented in yellow color in the Figure 8. They were then combined with the experimental enthalpy of reaction (discussed previously) and fitted thanks to the Gibbs equation (eq. 2) in order to find the three entropies of reaction (see Table 1). Finally, thermodynamic equilibriums of LaCl_3 are presented in the Figure 8. Our results, detailed hereinafter do not show convergence with any particular literature. Indeed, our results for the first dehydration step are close to those found thanks to the mathematical model, whereas, results for the second step show an agreement with Polyachenok’s experimental studies and the third decomposition reaction seems to be close to those of Sahoo et al [15], [16].

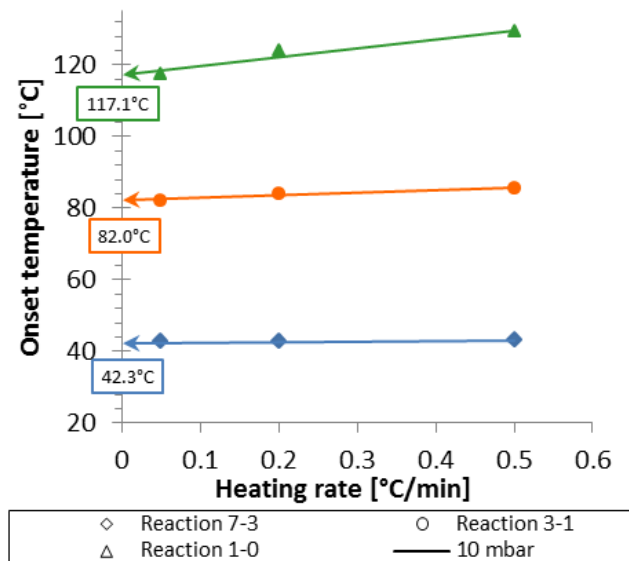


Figure 7: Dehydration temperature in [°C] with the dehydration rate in [°C/min] for the three step reactions of $\text{LaCl}_3\cdot 7\text{H}_2\text{O}$ decomposition at 10 mbar. Theoretical onset temperatures (at $0^\circ\text{C}/\text{min}$) are represented with an arrow on Y axis.

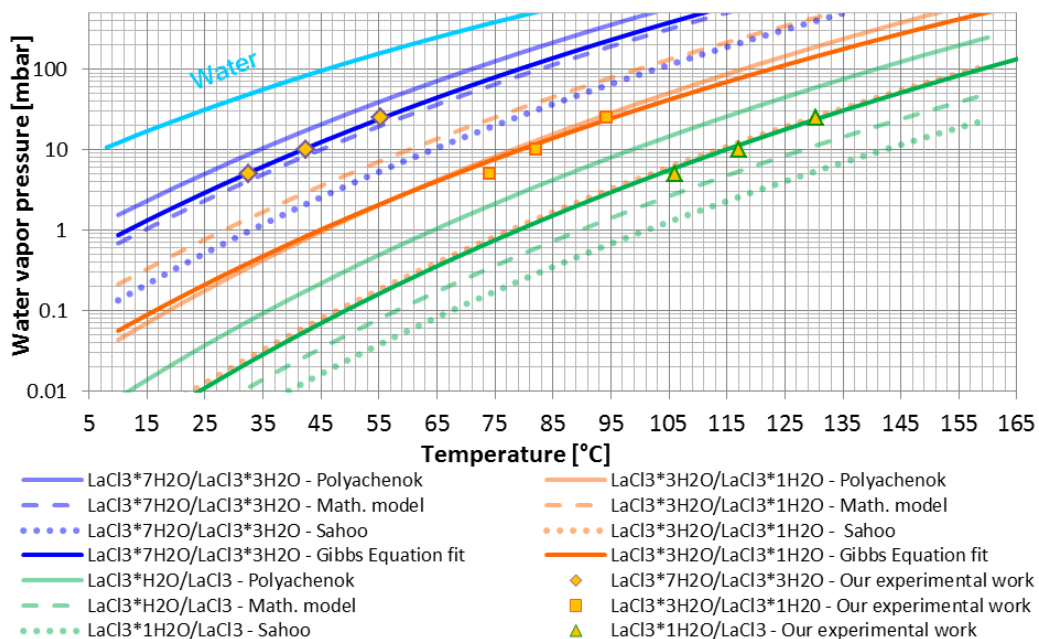


Figure 8: Thermodynamic diagram on LaCl_3 – literature and experimental work

Table 2: 'Real' onset temperature obtained for the three-step reaction at 5, 10 and 25mbar

Reaction step 'real onset temperature' [°C] Pressure [mbar]	$LaCl_3 \cdot 7H_2O$ $\rightarrow LaCl_3 \cdot 3H_2O + 4H_2O$	$LaCl_3 \cdot 3H_2O$ $\rightarrow LaCl_3 \cdot H_2O + 2H_2O$	$LaCl_3 \cdot H_2O \rightarrow LaCl_3$ $+ H_2O$
5	32.5	74.1	106
10	42.3	82	117.1
25	55.4	94.3	130.3

3. Large scale study of $LaCl_3$ – Thermochemical reactor with impregnated matrix

In order to improve heat and mass transfers inside the reactive material, a non-active ceramic porous matrix was considered in this paper. This matrix should enable salt crystals to be physically separated from each other and is expected to greatly enhance the effectiveness of our thermochemical reactor by contributing to the increase of energy released.

3.1 Design of the composite

The ceramic matrix used in this study was manufactured by 3D printing by MATEIS laboratory. More precisely, they were printed with robocasting, a technology which consists on the micro-extrusion of a paste in the three space directions. First, ceramic paste was formulated from hydrogel to guarantee a good printability. Then, ceramic paste was printed through a 400 μm diameter with a scaffold design. Finally, the final parts were obtained by a debinding and partial sintering step. Figure 9 shows the manufacturing by 3D printing and the final composite material.

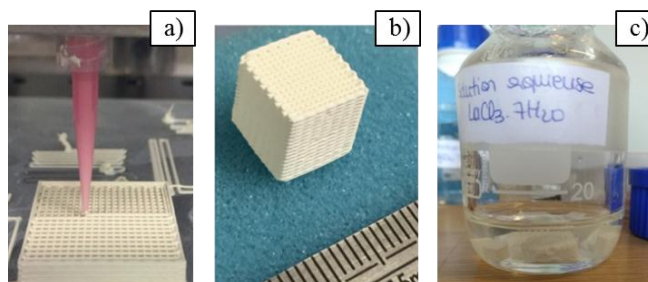


Figure 9: Ceramic porous matrix: a) 3D printing ; b) 2cm³ porous matrix ; c) Impregnation of matrix in a solution of $LaCl_3$

Some experimental campaigns were carried out in order to elaborate the composite material with salt hydrate impregnated into matrix. To anticipate the scale-up of the composite elaboration, it is important to determine the fastest and the most effective protocol which will impregnate the largest amount of salt in the shortest time. Whereupon, feasibility and strength tests were carried out on impregnated matrixes in order to define the best composite design. The first tests led to the determination of the optimal conditions of matrix impregnation with the largest amount of salt possible. In order to evaluate the percentage of impregnation of porous matrix depending on their characteristics, three parameters were tested: the impregnation time, the number of impregnation, and the initial porosity of the matrix. Concerning these three experimental campaigns, only $LaCl_3$ solution was used. For the test of the influence of the impregnation time, several matrixes were tested at different periods of impregnation varying from ten minutes to two hours. Regarding the study of the number of impregnations, only two successive impregnations were done and about the influence of the initial matrix porosity, two matrixes with of different compositions were compared (16% and 75% of porosity). Moreover, influence of the nature of salt hydrate was also investigated in order to evaluate if one salt from the three is better for this type of study. Three saturated salt solutions of were prepared with $LaCl_3$, $SrBr_2$ and $MgSO_4$. Solubility of each salt is presented in the Table 3 and expressed in gram of hydrated salt per gram of water. Matrixes were dived into one of the three salt solutions, during the same period of time before being heated.

Table 3: Salt hydrates solubility

Salt hydrate	Molar mass [g/mol]	Solubility in water (20°C): [g/g of water]
$LaCl_3 \cdot 7H_2O$	371	293,4g/100mL
$SrBr_2 \cdot 6H_2O$	355,5	71 g/100mL
$MgSO_4 \cdot 7H_2O$	120,37	107 g/100mL

After weighting-in with a microbalance (at 0,01g accuracy), each empty matrix was dived into a saturated salt solution. After impregnation (time depending of the case studied), impregnated matrixes were put on a heater and dehydrated at 150°C during about 5h. They were then weighed in order to evaluate the quantity of salt impregnated. The impregnation rate was expressed in percentage in function of the dehydrated mass, as it is detailed in the equation 6. Initial mass correspond to the mass of the empty matrix, i.e. before impregnation, whereas, dehydrated mass is the final mass of the matrix, after impregnation and heating.

$$\% \text{ impregnation} = \frac{\text{Dehydrated mass} - \text{Initial mass}}{\text{dehydrated mass}} \quad [\text{wt.}\%] \quad (\text{eq. 6})$$

Impregnation tests results are presented in the Table 4. For each experimental test, reproducibility was carried out. This is highlighted with the second subscript number in the matrix name. Good impregnation abilities for matrix with a high porosity rate (75%) are observed. The impregnation rate is around 61% after 30 min for this matrix, while it is 15.5% for the matrix with 16% of porosity. Furthermore, Table 4 shows that after 15 minutes, the increase of impregnation time does not allow a significantly increase of the impregnation rate. Thus after 15 minutes the impregnation rate is of 31% and is of 33% after 1h. Note that several impregnations have no significant impact. as a consequence of these results, the MATEIS laboratory succeeded in doing ceramic porous matrix with a higher porosity level at 85% and an impregnation time of 30 minutes has been chosen.

Table 4: Influence of the protocol of the matrix impregnation with LaCl₃

Influence tested	Matrix	Time	% Impregnation
Porosity 75%	M ₁	30 min	62.78
	M ₁₁		60.8
Porosity 16%	M ₂	30 min	15.15
	M ₂₂		16.09
Impregnation time	M ₃	15 min	31.23
	M ₃₃		30.21
	M ₄	30 min	32.82
	M ₄₄		32.04
	M ₅	1h	33.1
	M ₅₅		33.29
Number of impregnation	M ₆	10 + 10 min	32.2
	M ₇	20 min	26.7

Concerning the study of the influence of the type of salt, results presented in the Table 5 show a higher impregnation level (in percentage of weight) for the SrBr₂ and the LaCl₃ by following the equation 6. However, regarding the molar mass of each salt, MgSO₄ has a better impregnation level in percentage of mole per gram due to its low molar mass.

Table 5: Influence of the type of salt

Matrix	Time	% Impregnation (cf. eq 6)	% Impregnation (mol)/g
SrBr ₂	35 min	M1	40.38
		M11	38.29
MgSO ₄	35 min	M2	16.79
		M22	17.84
LaCl ₃	35 min	M3	34.1
		M33	35.74

Once impregnated, it was important to test the airflow resistance of these matrixes. An experimental campaign was carried out to evaluate the maximum flow-rate that can get through the matrix without damaging it or leading to a loss of material related to the separation of salt crystals with the matrix. A thermochemical reactor of few centimeters long was manufactured in 3D-printing. It was designed to host a ceramic matrix of 1cm² and variable thickness from 1mm to 1cm. Figure 10 presents the 3D-printed reactor with an impregnated ceramic matrix.

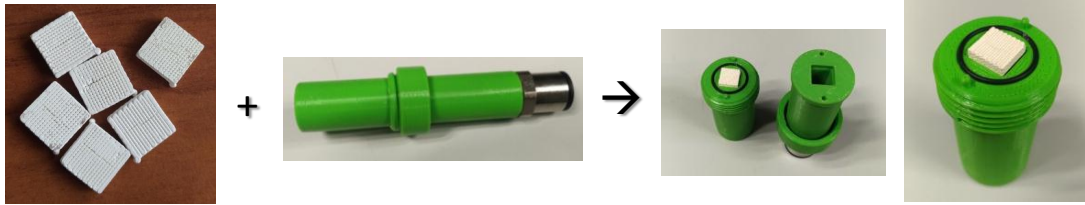


Figure 10: 3D-printed thermochemical reactor with 1cm² ceramic porous matrixes

An experimental bench test was set up to tests the 3D-printed thermochemical reactor with different matrixes impregnated from 20min to 2h. It is presented in the Figure 11. Two pressures sensors were installed upstream and downstream of the flowmeter. The flow rate passing through the matrix was controlled by the pressure set point upstream. The study was conducted for flow rate ranging from a few liters per minute to 400l/min. The study had shown conclusive results. No mass loss or destruction of the matrix was observed, which is encouraging for the next characterization studies.

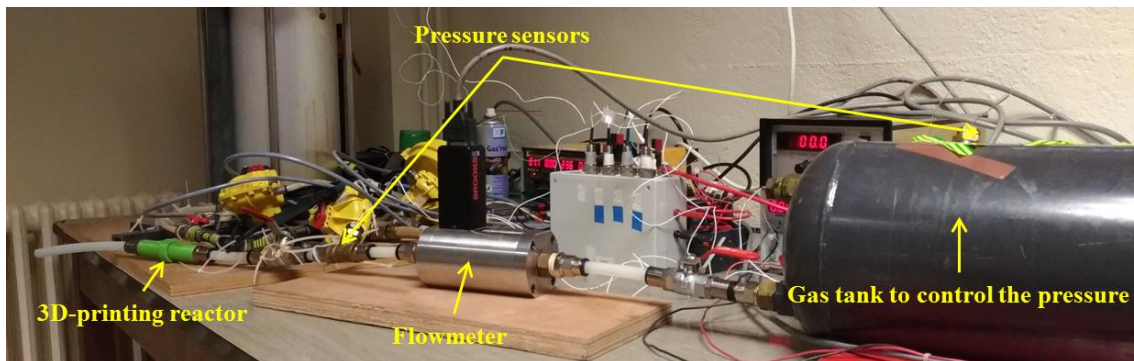


Figure 11: Experimental bench test for the maximal flow-rate test

3.2 Performances characterization of the LaCl₃ composite material

In order to characterize this composite material and to evaluate its thermal performances, a characterization bench test was set up. The variation of the moist air temperature at the reactor inlet and outlet was studied for different flow rate during the composite hydration. Firsts experiments were carried out on the 1cm² impregnated porous matrix thanks to the 3D-printed reactor. Then, these results were compared with salt bed for the same experimental conditions.

For these studies, experimental bench test was equipped of a humidifier in front of the thermochemical reactor (3D-printer or hydration column). The micrometer screw installed at the humidifier outlet was 100% open to allow a high relative humidity upstream of the reactor. Two thermocouples were installed on both sides of reactor, in order to be able to calculate the temperature variation between the inlet and the outlet of the system. Moreover, a humidity sensor was installed at the outlet of the reactor.

First series of tests were achieved with two different ceramic matrixes impregnated of LaCl₃. The first matrix studied was impregnated into a saturated salt solution of LaCl₃ during 1h40, which corresponds to a percentage of impregnation of 31.2% of mass; whereas, the second matrix was impregnated only 20 min for a mass impregnated at 20.8% of LaCl₃. For each matrix, several flow rates were successively tested from few liters per min to about 16l/min.

Results obtained on two different matrixes are presented in the Figure 12. The solid line in the Figure 12 represents the results of the tests carried out on the first matrix, and the dash line, those obtained with the second matrix. Results of the temperature variation between the inlet and the outlet of the thermochemical reactor, show that the ΔT increase when the flow rate decreases. It means that, the time spent by the moist air into the reactor seems to be too short and thus limiting. This phenomenon increases with the velocity. Finally, more the velocity is more the moist air to be heat is, with the same heat of reaction. Regarding the temperature variation for the first matrix, it can be noticed that the ΔT is very low for the highest flows, but regarding water vapor pressure ($P_{v_{out}}$), chemical reaction is still occurred because of the high humidity level at the outlet of the reactor. However, it is not the case for the second matrix: the outlet humidity level is very high, which means that there is much more channeling and preferential crossing in this matrix. Indeed, there is not enough salt impregnated in this second matrix and thus not sufficient contact between wet air and salt crystals.

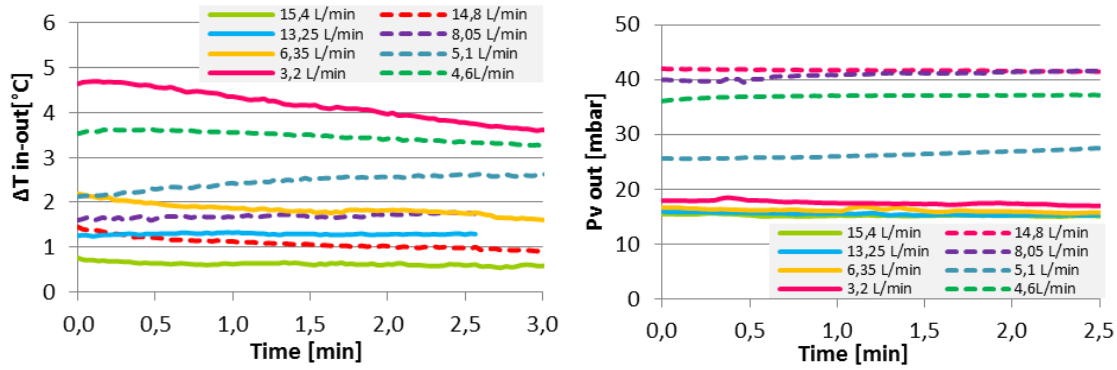


Figure 12: Variation of temperature in °C (left) and water vapor pressure $P_{v\ out}$ in mbar (right). The solid lines represent the matrix 1: 1h40 impregnated; the dash lines represent the matrix 2: 20min impregnated – Impregnated matrix in 3D-printed reactor

The second series of tests were carried out on $LaCl_3$ salt bed into a hydration column. Figure 13 presents the humidifier directly connected to the hydration column. For this experimental campaign, several amounts of salt (from 3mm to 15mm) were tested and for each one, several flow rates were successively passed through the hydration column from lowest to highest flow. In the same way as previously with the 3D-printed thermochemical reactor, the hydration column was connected on both sides with thermocouple and humidity sensors at the outlet of the column. A picture of the humidifier and the hydration column is presented in the Figure 13. Results of the different amounts of salt are almost similar, that is why only those obtained with 4mm amount of $LaCl_3$ salt hydrate were presented.



Figure 13: Humidifier and hydration column

For the first flow (i.e. the lowest) tested at 4mm, results show a variation of temperature higher of 3°C at the beginning of the chemical reaction, then the temperature variation drastically decrease in the salt reactive bed. This rapid rise in temperature followed by a sudden drop is quite typical of thermochemistry, especially for reactive salt bed in thermochemical reactor. Indeed, at the beginning, a lot of salt is ready to react at the same time. The chemical reaction seems to be very fast. After only the first two flow rates tested during about one minute each, there is already no longer temperature variation. It might be assumed that there is no longer chemical reaction either, but as it is showed in the Figure 14, the outlet water vapor pressure is low and it means that hydration is still occurring, but not enough to have a significant variation of temperature. Nevertheless, after mixing the salt bed, the same results as before were obtained, which means that all the salt did not react but just the first layer of the reactive bed. This last observation may highlight the possible agglomeration phenomenon and the need to impregnate salt crystal in porous matrix in order to prevent this phenomenon.

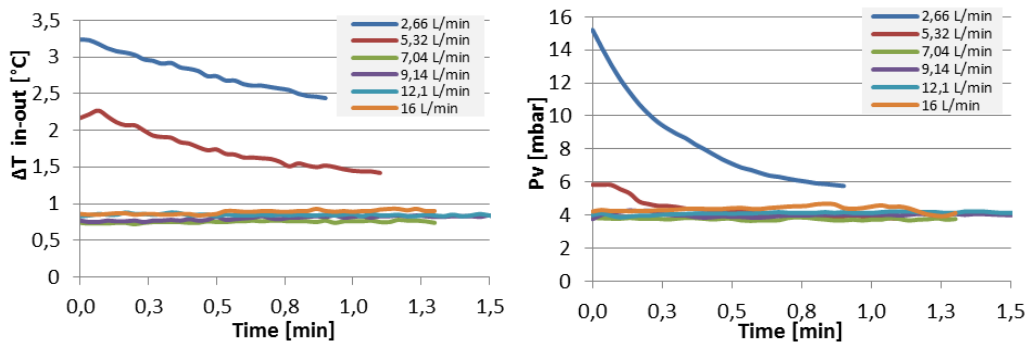


Figure 14: Temperature variation in °C (left) and water vapor pressure $P_{v\ out}$ in mbar (right) – 4mm Salt bed in hydration column

In order to conclude about these results on salt composites and ceramic matrix characterization, we can observe different issues impacting their thermal performances. Tests on impregnated matrix showed channeling problem into the matrix which led to pore contact between reactive salt and wet air, and highlighted the need to impregnate more salt in the matrix. Moreover, tests on reactive salt bed evidence the low variation of temperature into the reactive salt bed. Nevertheless, it is important to note that the two reactors were not isolated and thermal losses might not be negligible.

4. Conclusion and perspectives

LaCl₃ was two scales studied. First, the crystal's scale provides a better understanding of its thermodynamic properties. The thermodynamic study of the LaCl₃ showed that heating rate has an influence on the onset temperature. Indeed, the higher the dehydration rate, the lower the accuracy. The definition of the 'real' onset temperature by a graphic method yielded highly accurate results and allowed the definition of the thermodynamic diagram of this salt. Then, the extrapolation for the others couples (pressure / temperature) was done using the Gibbs equation. Our results were compared to those of the literature, obtained thanks to experimental and modeling studies. They showed convenient results with a mathematical model, especially for the first and the third thermochemical reactions (respectively from LaCl₃ heptahydrate to trihydrate and from LaCl₃ monohydrate to anhydrous form).

The second scale studied on LaCl₃ was about a technologic solution to avoid agglomeration phenomenon and increase heat and mass transfers in the reactive material. Ceramic porous matrixes were manufactured by the laboratory MATEIS to the objective of prevent and counteract this negative phenomenon. Design protocols were studied and showed that the fastest and the most effective way to impregnate ceramic porous matrix with salt hydrate is to dip the empty ceramic porous matrix into a salt-water solution during 30 minutes. Then, studies on two different thermochemical prototypes (one to test impregnated matrixes and the other a salt bed) highlighted the lack of salt into ceramic porous matrix because of their low surface and volume, and might evidence the agglomeration phenomenon into the reactive salt bed.

Based on these results, a bigger ceramic porous matrix (2cm³ of volume) was manufactured by 3D-printing by MATEIS laboratory. Another thermochemical reactor will be set up. Azote gas will be used as wet air to pass through the thermochemical reactor composed by the 2cm³ impregnated ceramic matrixes. To study the mass and enthalpy variations, the inlet gas temperature and humidity will be controlled and the outlet characteristics of the air will be measured. These results will be compared with those of literature and modeling studies. Moreover, in order to have a better understanding of the temperature field distribution in the thermochemical reactor, a germanium plate will be disposed on a lateral face. With an infrared camera, variations of the temperature field distribution within the reactor during the chemical process (sorption or desorption) will be seen. Likewise, a glass plate will be placed on the upper face of the reactor. Thanks to this plate, physical changes of crystalline structure during hydration or dehydration will be observed throughout the ceramic porous matrix. This study of the LaCl₃ at larger scales will allows access to the temperature distribution within the thermochemical reactor and will highlight temperature and humidity variations.

5. Acknowledgments

We would like to warmly thank the French laboratory: MATEIS at INSA Lyon, for the manufacture of the ceramic porous matrix and their daily work which aim to constantly optimize their structure to gain strength, the matrix size or the porosity of the material.

We would like to thank the French laboratory: Ampère at INSA Lyon for their help studying maximum flow rates during characterization studies.

We would also like to thank the French National Research Agency for the financial support provided to the project DECARTH ANR-16-CE22-0006-01 and to which this thesis is attached.

Nomenclature		Indices	
h	molar enthalpy, J/mol	eq	equilibrium
p	pressure, Pa	g	gas
R	gas constant, J/mol/K	in	inlet
T	temperature, K	out	outlet
Greeks symbols		Exponents	
Δh_r^0	standard enthalpy of reaction, J/(mol.s)	0	reference
ΔS_r^0	standard entropy of reaction, J/(mol.s)/K		
v	stoichiometric coefficient, molG/molS		

6. References

- [1] P. Tatsidjoudoug, N. Le Pierrès, et L. Luo, « A review of potential materials for thermal energy storage in building applications », *Renew. Sustain. Energy Rev.*, vol. 18, p. 327-349, févr. 2013.
- [2] J. Xu, R. Z. Wang, et Y. Li, « A review of available technologies for seasonal thermal energy storage », *Sol. Energy*, vol. 103, p. 610-638, mai 2014.
- [3] G. Alva, Y. Lin, et G. Fang, « An overview of thermal energy storage systems », *Energy*, vol. 144, p. 341-378, févr. 2018.
- [4] B. Michel, P. Neveu, et N. Mazet, « Comparison of closed and open thermochemical processes, for long-term thermal energy storage applications », *Energy*, vol. 72, p. 702-716, août 2014.
- [5] K. E. N'Tsoukpoe, H. Liu, N. Le Pierrès, et L. Luo, « A review on long-term sorption solar energy storage », *Renew. Sustain. Energy Rev.*, vol. 13, n° 9, p. 2385-2396, déc. 2009.
- [6] G. Krese, R. Koželj, V. Butala, et U. Stritih, « Thermochemical seasonal solar energy storage for heating and cooling of buildings », *Energy Build.*, vol. 164, p. 239-253, avr. 2018.
- [7] F. Trausel, A.-J. de Jong, et R. Cuypers, « A Review on the Properties of Salt Hydrates for Thermochemical Storage », *Energy Procedia*, vol. 48, p. 447-452, 2014.
- [8] A. Sharma, V. V. Tyagi, C. R. Chen, et D. Buddhi, « Review on thermal energy storage with phase change materials and applications », vol. 13, n° 2, p. 318-345, févr. 2009.
- [9] Q. Ma, L. Luo, R. Z. Wang, et G. Sauce, « A review on transportation of heat energy over long distance: Exploratory development », *Renew. Sustain. Energy Rev.*, vol. 13, n° 6-7, p. 1532-1540, août 2009.
- [10] K. E. N'Tsoukpoe, T. Schmidt, H. U. Rammelberg, B. A. Watts, et W. K. L. Ruck, « A systematic multi-step screening of numerous salt hydrates for low temperature thermochemical energy storage », *Appl. Energy*, vol. 124, p. 1-16, juill. 2014.
- [11] M. Richter, E.-M. Habermann, E. Siebecke, et M. Linder, « A systematic screening of salt hydrates as materials for a thermochemical heat transformer », *Thermochim. Acta*, vol. 659, p. 136-150, janv. 2018.
- [12] L. Scapino, H. A. Zondag, J. Van Bael, J. Diriken, et C. C. M. Rindt, « Sorption heat storage for long-term low-temperature applications: A review on the advancements at material and prototype scale », *Appl. Energy*, vol. 190, p. 920-948, mars 2017.
- [13] L. F. Cabeza, A. Solé, et C. Barreneche, « Review on sorption materials and technologies for heat pumps and thermal energy storage », *Renew. Energy*, vol. 110, p. 3-39, sept. 2017.
- [14] A. Fopah-Lele *et al.*, « Lab-scale experiment of a closed thermochemical heat storage system including honeycomb heat exchanger », *Energy*, vol. 114, p. 225-238, nov. 2016.
- [15] D. K. Sahoo, R. Mishra, H. Singh, et N. Krishnamurthy, « Determination of thermodynamic stability of lanthanum chloride hydrates (LaCl₃·xH₂O) by dynamic transpiration method », *J. Alloys Compd.*, vol. 588, p. 578-584, mars 2014.
- [16] O. G. Polyachenok, « Thermal stability and thermodynamics of LaCl₃ lowest hydrate, XVIII International Conference on Chemical Thermodynamics », Russia Samara, 2011.
- [17] R. J. Roy et G. J. Kipouros, « Estimation of vapour pressures of Neodymium trichloride hydrates », p. 15.
- [18] W. Judge et G. J. Kipouros, « Prediction of hydrogen chloride pressure to avoid hydrolysis in dehydration of dysprosium trichloride hexahydrate (DyCl₃·6H₂O) », *Can. Metall. Q.*, vol. 52, n° 3, p. 303-310, juill. 2013.
- [19] J.-P. Dumas *et al.*, « Interpretation of calorimetry experiments to characterise phase change materials », *Int. J. Therm. Sci.*, vol. 78, p. 48-55, avr. 2014.